Transplant International

ORIGINAL ARTICLE

Echocardiographic assessment of right heart function in heart transplant recipients and the relation to exercise hemodynamics

Tor Skibsted Clemmensen, Hans Eiskjær, Brian Bridal Løgstrup, Mads Jønsson Andersen, Søren Mellemkjær & Steen Hvitfeldt Poulsen

Department of Cardiology, Aarhus University Hospital, Skejby, Denmark

Correspondence
Tor Skibsted Clemmensen MD, Department of Cardiology, Aarhus University Hospital, Palle Juul-Jensens Boulevard 99, Skejby, 8200 Aarhus N, Denmark.
Tel: 0045 78452251;
fax: +45 7845 2260;
e-mail: torclemm@rm.dk

SUMMARY

This study aimed to characterize right heart function in heart transplantation (HTx) patients using advanced echocardiographic assessment and simultaneous right heart catheterization (RHC). Comprehensive two-dimensional (2D) and three-dimensional (3D) echocardiographic assessment of right heart function was performed in 105 subjects (64 stable HTx patients and 41 healthy controls). RHC was performed at rest and during semi-supine maximal exercise test. Compared with controls, in conclusion, HTx patients had impaired right ventricle (RV) systolic function in terms of decreased RV-free wall (FW) global longitudinal strain (GLS) ($-20 \pm 5\%$ vs. $-28 \pm 5\%$, $P < 0.0001$) and 3D-ejection fraction (EF) ($50 \pm 8\%$ vs. $60 \pm 6\%$, $P < 0.0001$). In HTx patients, echocardiographic RV systolic function was significantly correlated with NYHA-class (3D-RVEF: $r = -0.62$, $P < 0.0001$; RV-FW-GLS: $r = -0.41$, $P = 0.0009$) and cardiac allograft vasculopathy (3D-RVEF: $r = -0.42$, $P = 0.0005$; RV-FW-GLS: $r = -0.25$, $P = 0.0444$). RHC demonstrated a good correlation between invasively assessed resting RV-stroke volume index and exercise capacity ($r = 0.58$, $P < 0.0001$) and NYHA-class ($r = -0.41$, $P = 0.0009$). RV systolic function is reduced in HTx patients compared with controls. 3D RVEF and 2D longitudinal deformation analyses are associated with clinical performance in stable HTx patients and seem suitable in noninvasive routine right heart function evaluation after HTx. Invasively assessed RV systolic reserve was strongly associated with exercise capacity.

Transplant International 2016; 29: 909–920

Key words
3D echocardiography, cardiac allograft vasculopathy, exercise haemodynamics, global longitudinal systolic function, heart transplantation, right ventricular function

Received: 13 December 2015; Revision requested: 26 February 2016; Accepted: 2 May 2016; Published online: 7 July 2016

Introduction

Right ventricular (RV) failure is a serious complication in the immediate phase after heart transplantation (HTx) and accounts for approximately 50% of all early complications following HTx [1,2]. Pretransplant elevated pulmonary vascular resistance is widely recognized as the most prominent risk factor for acute RV dysfunction [3–5]. During the first years after HTx, the donor heart adapts to the altered systemic and pulmonary

doi:10.1111/tri.12793

vascular loading conditions and metabolic demands. During this period, emergence of cardiac allograft vasculopathy (CAV) and rejection episodes may lead to impaired perfusion and fibrosis development subsequently impairing RV function. Hence, RV function alterations are of clinical importance, but RV anatomy challenges function and size assessment with conventional two-dimensional (2D) echocardiography. Several studies have therefore explored RV function in HTx patients using 2D tissue Doppler echocardiography, and they describe reduced RV systolic function in both the immediate and the long-term post-transplant period [6–8]. Three-dimensional (3D) RV ejection fraction (RVEF) assessment has emerged as a reliable method for global RV function assessment [9]. Recently, 2D-speckle tracking echocardiography (2D-STE) applied on RV (RV global longitudinal strain, RV-GLS) has shown important prognostic value in various cardiac diseases [10–14]. However, neither RV-GLS nor 3D-RVEF has been evaluated in HTx patients with respect to CAV, rejection burden, and hemodynamics. Hence, the clinical significance of these imaging modalities remains unknown.

Thus, this present study aimed to characterize RV function in stable HTx patients by 2D-STE and 3D full-volume RVEF with reference to clinical performance, exercise capacity, and exercise hemodynamics.

Methods

Patients

The study population consisted of 105 subjects (64 stable HTx patients and 41 controls) who were enrolled from September 2013 through October 2015. Patients ≥18 years of age had no severe valve disease and were included after having provided written informed consent according to the principles of the Helsinki Declaration. The healthy controls received no medication and had no cardio-pulmonary symptoms. The local scientific ethical committee of the Central Denmark Region approved the study. The study was registered with clinicaltrials.gov (NCT02077764).

Invasive hemodynamic measurements

Right heart catheterization (RHC) was performed in all HTx patients and in 13 controls. A standard 7.5-F triple lumen Swan-Ganz thermistor and balloon-tipped catheter (Edwards Lifesciences, Irvine, CA, USA) was used. The catheter was introduced into the right jugular vein under ultrasound guidance using the Seldinger technique [15], and using advanced pressure waveform and fluoroscopy, it was guided into the pulmonary artery (PA). Pulmonary capillary wedge pressure (PCWP), mean right atrial pressure (mRAP), systolic and diastolic PA pressure (sPAP, dPAP), mean PA pressure (mPAP), transpulmonary gradient (TPG = mPAP −PCWP), cardiac output (CO), and blood pressure (BP) were measured at rest, at each exercise level until exhaustion, and 5 min postexercise. Based on previous studies of healthy controls, we considered a resting mPAP exceeding 20 mmHg and/or 30 mmHg during exercise to be abnormal [16].

Cardiac output was measured by thermodilution by averaging two measurements not differing more than 10%. CO was indexed to body surface area (BSA) as cardiac index (CI). Stroke volume index (SVI) was calculated as CI divided by heart rate (HR). Pulmonary artery compliance (PAC) was calculated as: SV/(sPAP−dPAP). Pulmonary vascular resistance index (PVRI) was calculated as: PVRI = 80 × (mPAP−mPCWP)/CI. Systemic vascular resistance index (SVRI) was calculated as: SVRI = 80 × (mean arterial pressure (MAP)−mRAP)/CI. Oxygen consumption (VO_2) was calculated using the indirect Fick by: VO_2 = CO × arteriovenous oxygen difference × 1.36 × hemoglobin (g/dl) × 10. Arteriovenous oxygen content difference was measured as the difference between pulsoxymetrie measurements and directly measured PA O_2 content at rest and peak exercise. RV stroke work index (RVSWI) was calculated as: RVSWI = SVI × 0.0136 × (mPAP−mRAP).

Exercise protocol

All subjects performed a multistage symptom–limited, semi-supine bicycle exercise test using the Echo Cardiac Stress Table (Lode B.V., Groningen, the Netherlands). Workload started at 0 W and was increased by 25 W every 3 min. Patients and controls were encouraged to maintain a fixed pedaling speed of 60 rounds per minute and to exercise until exhaustion (Borg > 18) [17]. Exercise capacity is expressed as metabolic equivalent of task (METs), calculated using the equation: METs = (1.8 × ((peak Watt × 6.12 kg/min/body weight in kg) + 7)/3.5.

Echocardiography

Echocardiography was performed using a commercially available ultrasound system (Vivid 9, GE Healthcare, Horten, Norway) with a 3.5-MHz-phased array

transducer (M5S) for 2D evaluation and a 4V-D transducer for 3D evaluation.

Patients and controls underwent a comprehensive echocardiographic assessment according to current guidelines [9]. Using 2D-STE RV-GLS was assessed from a modified four-chamber view. We calculated both RV-GLS averaging 6 segments and RV free-wall-GLS (RV-FW-GLS) averaging the 3 lateral segments. The RV-GLS and RV-FW-GLS magnitudes were assessed from frame-by-frame speckle patterns tracking throughout the left-sided myocardium in standard 2D cine-loops with a frame rate >55 frames/s. The speckle area of interest was manually adjusted to obtain optimal tracking results. Segments with unacceptably low tracking quality were excluded.

Tricuspid annular systolic velocity wave (RV-S′) was assessed by lateral, pulsed tissue Doppler velocities. Likewise, tricuspid annular plane systolic excursion (TAPSE) was measured from the lateral tricuspid plane.

3D RV-EF and 3D LV-EF were obtained by sampling six heartbeats during breath-hold aiming at a frame rate >25 frames/s. RV systolic function parameters are presented in Fig. 1.

Data were analyzed offline using dedicated software (EchoPAC PC SW-Only, 113, GE-Healthcare, Milwaukee, WI, USA and TomTec 4D RV-function, Munich, Germany) by a single investigator (TSC) blinded to clinical status and invasive measurements.

Coronary angiography

Coronary arteries were imaged in two planes after administering intracoronary nitroglycerin (200 μg). At least two projections of each coronary artery were acquired. All three major branches were analyzed offline using 2D quantitative coronary angiography (2D-QCA). Maximal stenosis of each vessel was calculated using a proximal and distal reference area. CAV was classified according to the International Society of Heart and Lung Transplantation (ISHLT) guidelines [18].

Endomyocardial biopsy

Previous acute cellular rejection episodes were histopathologically graded in three forms, according to ISHLT guidelines [19], and rejection scores were calculated as previously described [20].

Statistical methods

Normally distributed data are presented as mean ± standard deviation (SD), non-normally distributed are

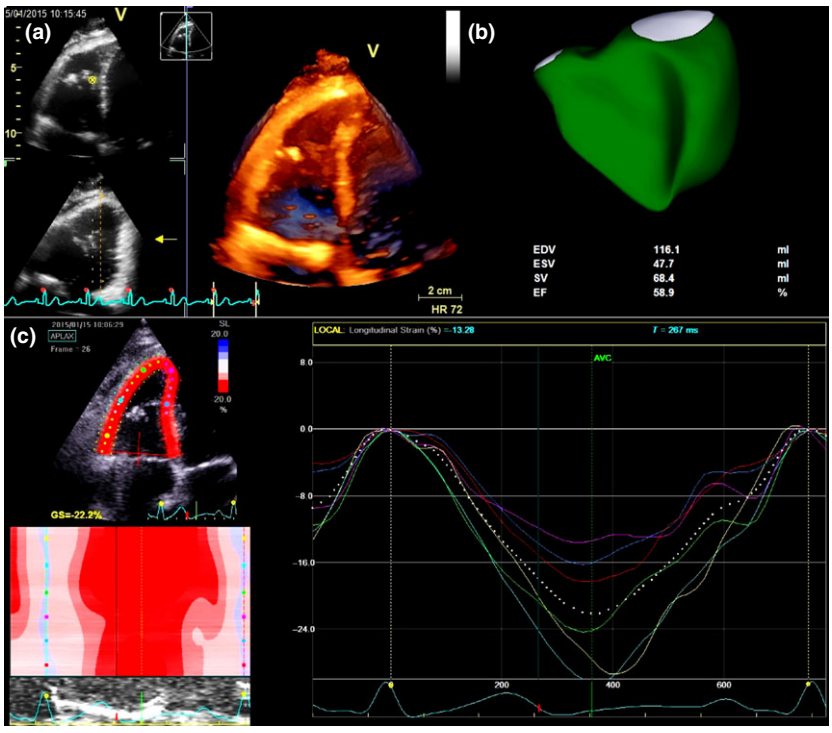

Figure 1 Echocardiographic modalities used to characterize RV systolic function. (a) 3D full volume raw images; (b) 3D model of RV based on full volume images; (C) 2D speckle tracking of RV.

presented as median and interquartile range (IQR). Categorical data are presented as absolute values with percentages. Histograms and Q-Q-plots were used to check continuous values for normality. Between-group differences were assessed by t-test for normally distributed data and Mann–Whitney *U*-test for non-normally distributed data. Pearsons correlation coefficient was calculated for normally distributed data and Spearman correlation coefficient for non-normally distributed data. Echocardiographic parameters were adjusted for total number of echocardiographic hypothesis tests performed in the study using the Šidák-Holm (SH) multiplicity correction of *P*-values. Likewise, hemodynamic parameters were adjusted for total number of hemodynamic hypothesis tests performed in the study. Finally, correlations between echocardiographic parameters and hemodynamic parameters were adjusted for total number of correlations performed in the study. *P*-values are presented as unadjusted values and SH multiplicity corrected *P*-values. All tests were two-sided, and $P < 0.05$ was considered statistically significant. Analyses were performed using STATA (STATA/IC 13, StataCorp LP, College Station, TX, USA).

Results

Patient characteristics

Table 1 displays the clinical characteristics of the patients. Sixty-four HTx patients were included with a

Table 1. Patient characteristics.

	HTx patients (n = 64)	Controls (n = 41)	P value
Male, (%)	73%	59%	0.11
Donor age (years)	42 ± 12		
Age (years)	53 ± 13	51 ± 12	0.30
Time since transplantation (years)	8 ± 6		
Pretransplant PVR (Wood units)*	2.0 ± 0.7		
NYHA functional class >1, (%)	27%		
Body mass index (kg/m^2)	25 ± 4	24 ± 2	0.07
Diabetes, (%)	17%		
Hypertension, (%)	88%		
CAV and previous rejections			
Graft vasculopathy, (%)	61%		
Previous percutaneous intervention	16%		
Maximal stenosis by 2D QCA (%)	44 ± 27		
Number of EMBs showing 1R	7.5 ± 4.1		
Number of EMBs showing ≥2R	0.8 ± 1.1		
Rejection score	9.4 ± 5.4		
Medication			
Prednisolone, (%)	42%		
Cyclosporine, (%)	38%		
Tacrolimus, (%)	63%		
Mycophenolate, (%)	76%		
Everolimus, (%)	28%		
Statins, (%)	87%		
ACE/ATII inhibitor, (%)	73%		
Calcium-blocker (%)	46%		
Furosemide or bumetanide, (%)	21%		
Thiazid, (%)	24%		
Biochemistry			
Creatinine (μmol/l)	104 [80;129]		
Hemoglobin (mM)	8.5 [7.7;9.1]		
Troponin-T (ng/l)	11 [5;21]		
NT-ProBNP (ng/l)	342 [192;922]		

PVR, pulmonary vascular resistance; NYHA, New York Heart Association; EMB, endomyocardial biopsy.

Data are presented as percent or mean ± standard deviation or median and [IQR].

*Data available from 43 of 64 patients.

Transplant International 2016; 29: 909–920

Table 2. Right ventricle systolic and diastolic function by echocardiography in HTx patients and healthy controls.

	HTx (n = 64)	Controls (n = 41)	P-value
Noninvasive hemodynamics			
MAP rest (mmHg)	101 ± 12	91 ± 11	**<0.0001***
MAP peak stress (mmHg)	126 ± 16	125 ± 16	0.64
HR rest (beats/min)	84 ± 13	62 ± 7	**<0.0001***
HR peak stress (beats/min)	132 ± 17	148 ± 18	**<0.0001***
Diastolic RV function			
TV-E	61 ± 18	48 ± 9.0	**<0.0001***
TV-A	37 ± 10	27 ± 6	**<0.0001***
TV-E-deceleration time (ms)	169 ± 48	251 ± 91	**<0.0001***
TV-e′	8 ± 2	10 ± 2	**<0.0001***
TV-E/e′ (ratio)	11 ± 7	5 ± 1	**<0.0001***
RA volume (ml/m^2)	26 ± 14	24 ± 8	0.45
Systolic RV function			
TR gradient (mmHg)	26 ± 7	21 ± 5	**0.0092**
TAPSE (cm)	1.4 ± 0.4	2.7 ± 0.4	**<0.0001***
3D RV-EF (%)	50 ± 8	60 ± 6	**<0.0001***
3D RV-EDV (ml)	113 ± 32	130 ± 32	**0.0071**
3D RV-ESV (ml)	57 ± 21	53 ± 18	0.36
3D RV-SV (ml)	56 ± 16	77 ± 18	**<0.0001***
RV-S′ (cm/s)	7 ± 2	12 ± 2	**<0.0001***
Free wall RV-GLS (%)	−20 ± 5	−28 ± 5	**<0.0001***
RV-GLS (%)	−18 ± 4	−25 ± 3	**<0.0001***

SBP, systolic blood pressure; MAP, mean arterial pressure; HR, heart rate; METs, metabolic equivalent of task; RA, right atrial; TV, tricuspid valve; AT, acceleration time; ET, ejection time; TR, tricuspid regurgitation gradient; TAPSE, tricuspid annular plane systolic excursion; RV, right ventricle; EF, ejection fraction; EDV, end diastolic volume; ESV, end systolic volume; SV, stroke volume; GLS, global longitudinal strain.

*Statistical significant after Šidák-Holm multiplicity correction.

mean transplant age of 8.1 years. Seven patients were operated by biatrial technique and 57 patients by bicaval technique. Sixty-one percent of the patients had CAV and 28% (18/64) of the patients had severe CAV (ISHLT class 2–3). Percutaneous intervention was previously performed in 10 patients.

Echocardiographic assessment of RV function in HTx patients and controls

The echocardiographic parameters of the HTx patients and the controls are presented in Table 2. The RV diastolic function parameters were impaired in HTx subjects with reduced deceleration time ($P < 0.0001$, SH-adjusted: $P = 0.0024$) and elevated RV E/e' ratio ($P < 0.0001$, SH-adjusted: $P = 0.0024$), while RA volume did not differ significantly (26 ± 14 ml/m^2 vs. 24 ± 8 ml/m^2, $P = 0.45$) between HTx patients and controls.

RV systolic function was lower in HTx patients compared with controls, Fig. 2. None of the controls had 3D RVEF < 45%, whereas 15 HTx patients (23%) had 3D RVEF < 45%. Despite significantly reduced stroke volume, CO based on 3D echocardiographic RV volume measurement (SV*HR) did not differ significantly between HTx patients and controls (4.7 ± 1.4 l/min vs. 4.8 ± 1.3 l/min, $P = 0.72$). A significantly higher tricuspid regurgitation gradient (TR-gradient) was noted in the HTx group than in the control group ($P = 0.0092$, SH-adjusted: $P = 0.0487$).

Relation between echocardiographic assessment of RV systolic and diastolic function and invasive hemodynamics at rest in HTx patients

A week correlation between RV systolic function by echocardiography and RV SVI derived from thermodilution was noted (3D RVEF: $r = 0.41$, $P = 0.0007$, SH-adjusted: $P = 0.0256$; RV-FW-GLS: $r = 0.24$, $P = 0.06$).

We found no correlation between resting RV diastolic Doppler filling parameters (RV-E/A-ratio, RV-E/e′-ratio, and RV-E-deceleration time) and resting invasive hemodynamics (mRAP and mPAP). RA volume was weakly

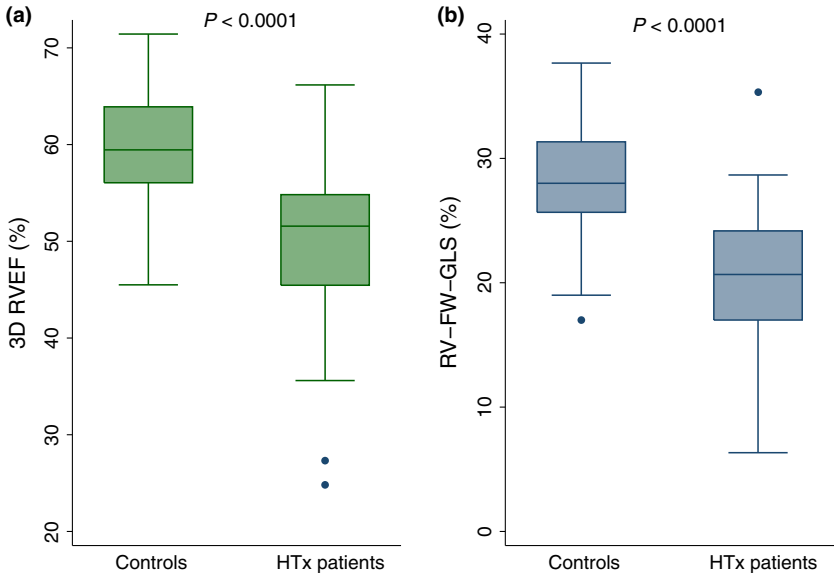

Figure 2 Box-plots with wiskers and *t*-tests comparing controls with heart transplanted patients regarding: (a) 3D right ventricular ejection fraction (3D RVEF); (b) Right ventricular global longitudinal strain-free wall (RV-FW-GLS).

correlated with mRAP ($r = 0.34$, $P = 0.0055$, SH-adjusted: $P = 0.16$). We found a moderate relation between the TR gradient and mRAP ($r = 0.30$, $P = 0.0289$, SH-adjusted: $P = 0.53$), mPAP ($r = 0.58$, $P < 0.0001$, SH-adjusted: $P = 0.0041$), and PAC ($r = -0.43$, $P = 0.0013$, SH-adjusted: $P = 0.0433$).

Invasive hemodynamics during exercise

Table 3 displays invasive hemodynamics at rest and during exercise in the HTx and control populations. We found that the exercise capacity was 39% lower in the HTx group than in the control group (5.9 ± 1.4 METs vs. 9.7 ± 1.7 METs, $P < 0.0001$, SH-adjusted: $P = 0.0041$).

At rest, LV and RV filling pressures in both groups were within normal range. However, HTx patients had significantly reduced CI and PAC. Furthermore, SVRI, PVRI, and PAP were significantly higher in HTx patients than controls.

With exercise, LV ($P < 0.0001$, SH-adjusted: $P = 0.0041$) and RV ($P < 0.0001$, SH-adjusted: $P = 0.0041$) filling pressures and RV stroke work ($P < 0.0001$, SH-adjusted: $P = 0.0041$) increased significantly, whereas PVRI ($P < 0.0001$, SH-adjusted: $P = 0.0041$) and PAC ($P = 0.0022$, SH-adjusted: $P = 0.0261$) decreased significantly in HTx patients. The increase in LV and RV filling pressures was significantly higher in HTx patients than in controls. No difference in RAP between rest and peak was seen in healthy controls ($P = 0.76$). Thermodilution-derived RV cardiac index increased by more than twofold in HTx patients ($P < 0.0001$, SH-adjusted: $P = 0.0041$) mediated by both increasing RV stroke volume ($P < 0.0001$, SH-adjusted: $P = 0.0041$) and HR ($P < 0.0001$, SH-adjusted: $P = 0.0041$). Still, peak exercise cardiac index was 36% lower in HTx patients than controls (6.0 ± 1.6 l/min/m^2 vs. 9.4 ± 1.5 l/min/m^2, $P < 0.0001$, SH-adjusted: $P = 0.0041$).

In the HTx patients, we found a strong relation between peak exercise METs and RV systolic reserve capacity measured by ΔCI ($r = 0.68$, $P < 0.0001$, SH-adjusted: $P = 0.0041$), ΔSVI ($r = 0.58$, $P < 0.0001$, SH-adjusted: $P = 0.0041$), ΔVO_2 ($r = 070$, $P < 0.0001$, SH-adjusted: $P = 0.0041$), and ΔHR ($r = 0.52$, $P < 0.0001$, SH-adjusted: $P = 0.0041$). We divided HTx patients into three METs groups (lower quartile, median group, and upper quartile). Peak exercise cardiac index increased significantly with the increase in METs. At rest, we found a very good correlation between RV SVI and HR ($r = -0.76$, $P < 0.0001$, SH-adjusted: $P = 0.0041$), but the relation disappeared with exercise ($P = 0.14$), Fig. 3.

In contrast to RV systolic capacity, alterations in RA filling pressure did not correlate with peak exercise METs (ΔRAP: $r = -0.04$, $P = 0.76$).

Clinical implications and determinants of RV function in HTx patients

We divided HTx patients into two groups based on a cutoff point of 3D RVEF above/below 45%. Forty-nine patients had normal RVEF and 15 patients reduced

Table 3. Invasive hemodynamics at rest versus peak exercise.

	Rest			Peak exercise		
	HTx (n = 64)	Controls (n = 15)	P-value	HTx (n = 63)	Controls (n = 14)	P-value
Peak exercise METs (ml/kg/min)				5.9 ± 1.4	9.7 ± 1.7	**<0.0001***
AV-diff (%)	28 ± 5	23 ± 3	**<0.0001***	66 ± 11	67 ± 6	0.90
SVRI (dynes/s/cm^5/m^2)	2925 ± 584	2197 ± 440	**<0.0001***	1604 ± 463	999 ± 148	**<0.0001***
CI (l/min/m^2)	2.7 ± 0.4	3.2 ± 0.5	**0.0001***	6.0 ± 1.6	9.4 ± 1.5	**<0.0001***
VO_2 (l/min)	265 ± 52	255 ± 55	0.50	1426 ± 560	2163 ± 392	**0.0002***
Stroke volume index (ml/m^2)	33 ± 8	50 ± 10	**<0.0001***	46 ± 12	61 ± 6	**<0.0001***
mRAP (mmHg)	5 ± 3	5 ± 2	0.91	14 ± 8	5 ± 5	**0.0008***
mPAP (mmHg)	19 ± 6	15 ± 2	**0.0340**	36 ± 7	26 ± 7	**<0.0001***
mPCWP (mmHg)	10 ± 5	8 ± 2	0.27	25 ± 9	14 ± 7	**0.0001***
TPG (mmHg)	9 ± 4	7 ± 1	**0.0369**	11 ± 6	12 ± 3	0.63
PVRI (dynes/s/cm^5/m^2)	262 ± 162	169 ± 39	**0.0011***	174 ± 119	97 ± 23	**0.0108**
PAC (ml/mmHg)	5.6 ± 2.3	8.8 ± 2.3	**<0.0001***	4.6 ± 2.9	7.3 ± 1.7	**<0.0001***
RV stroke work index (gm-m/m^2/beat)	6.2 ± 2.2	7.2 ± 1.3	**0.0080**	13.7 ± 6.1	18.6 ± 4.3	**0.0330**

AV-diff, arterial-venous saturation difference; SVRI, systemic vascular resistance index; CO, cardiac output; CI, cardiac index; VO_2, oxygen consumption; mRAP, mean right atrial pressure; mPAP, mean pulmonary arterial pressure; mPCWP, mean pulmonary capillary wedge pressure; TPG, transpulmonary pressure gradient; PVRI, pulmonary vascular resistance index; PAC, pulmonary arterial compliance; RV, right ventricle.

Data are presented as mean ± standard deviation.

*Statistical significant after Šidák-Holm multiplicity correction.

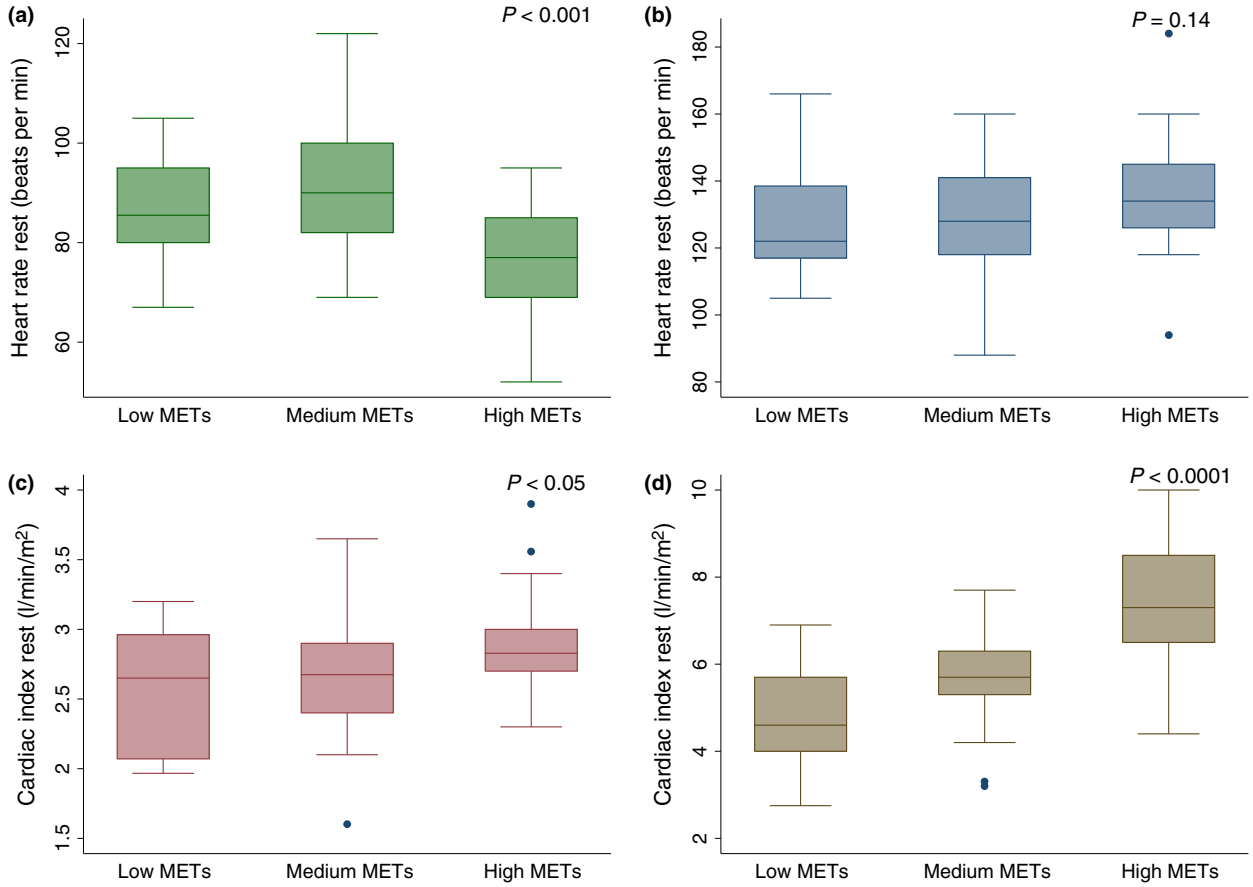

Figure 3 Box-plots with wiskers and ANOVA tests comparing heart transplanted patients divided into three groups based on metabolic equivalent of task (METs) regarding: (a) Heart rate at rest; (b) heart rate at peak exercise; (c) cardiac index at rest; (d) cardiac index at peak exercise. Low METs = lower quartile; medium METs = medium quartiles of METs; high METs = upper quartile.

RVEF. Patients with reduced RVEF had experienced significantly more treatment demanding acute cellular rejection episodes (≥2R) than patients with normal RVEF (1.3 ± 1.4 vs. 0.6 ± 0.9 episodes, $P = 0.0388$, SH-adjusted: $P = 0.15$). Furthermore, the severity of CAV was much more pronounced in the reduced RVEF group than seen in the normal RVEF group (2D QCA: reduced RVEF 64 ± 31% vs. 36 ± 21%, $P = 0.0002$, SH-adjusted: $P = 0.0024$).

Clinical, functional, and hemodynamic parameters associated with RV systolic function are presented in Table 4. No correlation was seen between pretransplant PVR and RV systolic function parameters. We found that RV systolic function was significantly correlated with previous rejection burden (3D RVEF: $P = 0.0341$, SH-adjusted: $P = 0.53$; RV-FW-GLS: $P = 0.0024$, SH-adjusted: $P = 0.08$) and with CAV severity (3D RVEF: $P = 0.0005$, SH-adjusted: $P = 0.0193$; RV-FW-GLS: $P = 0.0444$, SH-adjusted: $P = 0.57$). Furthermore, we noted a significant correlation between RV systolic function and NYHA functional class, Fig. 4.

We found a strong relation between LV and RV 3D EF ($r = 0.68$, $P < 0.0001$, SH-adjusted: $P = 0.0024$) and LV and RV stroke volume ($r = 0.65$, $P < 0.0001$, SH-adjusted: $P = 0.0024$). As 3D RVEF, 3D LVEF was only weakly correlated with exercise capacity ($r = 0.33$, $P = 0.0075$, SH-adjusted: $P = 0.0487$).

In contrast to the echocardiographic diastolic parameters, we found that NT-ProBNP was significantly correlated with resting values of mRAP ($r = 0.58$, $P < 0.0001$, SH-adjusted: $P = 0.0041$) and mPCWP ($r = 0.53$, $P < 0.0001$, SH-adjusted: $P = 0.0041$) in HTx patients.

Discussion

Our study demonstrates that RV systolic function is significantly reduced in HTx patients compared with healthy controls as assessed by conventional echocardiography, myocardial deformation imaging, and 3D RVEF. Importantly, reduced 3D RVEF is significantly related with increasing NYHA functional class and

Table 4. Bivariate correlation coefficients in the HTx population.

	TAPSE		RV-S′-lat		RV-GLS-lat		3D RV-EF		TR gradient	
	*r**	*P*-value	*r**	*P*-value	*r**	*P*-value	*r**	*P*-value	*r**	*P*-value
Clinical characteristics										
Maximal stenosis†	−0.30	**0.0156**	−0.29	**0.0233**	−0.25	**0.0444**	−0.42	**0.0005‡**	0.22	0.12
Rejection score	−0.23	0.08	−0.23	0.08	−0.39	**0.0024**	−0.28	**0.0341**	0.10	0.49
NYHA-class	−0.41	**0.0009‡**	−0.33	**0.0079**	−0.41	**0.0007‡**	−0.62	**<0.0001‡**	0.24	0.08
Resting hemodynamics										
RV-SVI	0.27	**0.0320**	0.28	**0.0286**	0.24	0.06	0.41	**0. 0007‡**	−0.24	0.08
mRAP (mmHg)	−0.24	0.06	−0.27	**0.0301**	−0.31	**0.0117**	−0.25	**0.0433**	0.30	**0.0289**
mPAP (mmHg)	−0.18	0.15	−0.15	0.26	−0.27	**0.0288**	−0.41	**0.0008‡**	0.58	**<0.0001‡**
PVRI	−0.26	**0.0437**	−0.26	**0.0404**	−0.14	0.26	−0.15	0.25	0.27	0.05
PAC	0.16	0.22	0.08	0.56	0.01	0.97	0.29	**0.0208**	−0.43	**0.0013‡**

NYHA, New York Heart Association; SVI, stroke volume index; mRAP, mean right atrial pressure; mPAP, mean pulmonary arterial pressure; PVRI, pulmonary vascular resistance index; PAC, pulmonary arterial compliance; RV, right ventricle; TAPSE, tricuspid annular plane systolic excursion; EF, ejection fraction; GLS, global longitudinal strain; TR, tricuspid regurgitation gradient.

*Data are presented as Pearson correlation coefficient test for normally distributed data or Spearman correlation coefficient test non-normally distributed data.

†Assessed by 2D-Quantitative coronary angiography.

‡Statistical significant after Šidák-Holm multiplicity correction.

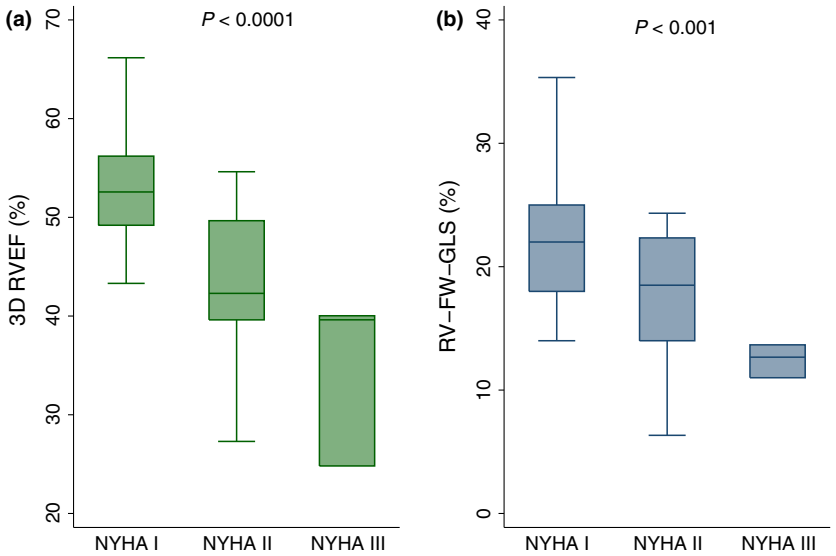

Figure 4 Box-plots with wiskers and ANOVA tests comparing heart transplanted patients divided into three groups based on New York Heart Association (NYHA) functional class. (a) 3D right ventricular ejection fraction (3D RVEF); (b) Right ventricular global longitudinal strain-free wall (RV-FW-GLS).

exercise capacity. Furthermore, previous rejection burden and CAV was significantly associated with reduced RV systolic function. Finally, we found that exercise capacity was strongly linked to invasively assessed RV systolic reserve capacity, but not to right heart filling pressures in a stable HTx patient cohort.

In this present study, we found reduced RV systolic function in long-term HTx patients, measured not only by tissue Doppler and TAPSE, but also by 3D RVEF and longitudinal deformation analysis. The echocardiographic parameters of RV systolic function used in this study offer different information regarding right heart systolic performance. Assessment of RVEF by 3D gives information about the global systolic RV function. The clinical value of 3D RVEF is seen notably after cardiac surgery where conventional measures of longitudinal RV function, such as TAPSE and RV-S′, are generally reduced and may not be representative of the overall

RV performance [9,21,22]. Hence, 3D RVEF assessment seems more reliable, when properly performed, than traditional surveillance by TAPSE and RV-S'. TAPSE and RV-S' are well-established methods and easy to perform, but they do not reflect the global function. Furthermore, the utility of TAPSE and RV-S' is limited by the angle-dependent nature of these parameters and the likely influence of the open-heart surgery. RV-GLS is a direct longitudinal myocardial deformation measure, angle-independent, and less confounded by overall heart motion [9]. However, 2D RV-GLS only partially reflects global RV function. Nevertheless, RV-GLS gives important prognostic value in heart failure patients, amyloidosis, pulmonary hypertension, and ischemic heart disease [10–14], but the prognostic role in HTx patients should be evaluated.

We found that 3D RVEF was significantly associated with both NYHA functional class and exercise capacity. This indicates that a global right heart function evaluation seems to provide important clinical information and may give incremental value to traditional echocardiographic RV function surveillance in HTx patients. D'Andrea and colleagues have previously studied RV systolic function in HTx patents. They found a good correlation between 3D RVEF by cardiac MRI and 3D echocardiography ($r = 0.89$, $P < 0.0001$). In contrast to our findings, D'Andrea and colleagues found no difference in 3D RVEF between rejection-free HTx patients and healthy controls [23]. However, in accordance with this present study, Wahl and colleagues demonstrated significantly reduced 3D RVEF by cardiac MRI in HTx patients surviving beyond 2 years [3].

In our study, we found a strong relation between LV and RV systolic function measured by 3D global EF. This indicates that RV function declines partially parallel with LV function in HTx patients. However, the observed reduced RV systolic function and exercise capacity in HTx patients is likely multifactorial. It is well-known that cardiac surgery leads to reduced LV and RV longitudinal function [21,22]. Previous studies have shown that TAPSE is significantly reduced during ACR [24] and affected by the cumulative number of previous ACR episodes [25]. These findings were supported and expanded by this present study in which we found a significantly higher burden of previous ACR episodes in patients with reduced 3D RVEF. The persistence of RV dysfunction after resolved ACR episodes may therefore be an important contributor to the lack of physical capacity in long-term HTx patients. In our study, the presence of CAV was significantly associated with reduced RV systolic function, indicating that perfusion abnormalities and/or myocardial RV scarring may be of importance. Butler and colleagues demonstrated significant prognostic value of myocardial scarring, RVEF, and RV volumes by CMR in HTx patients [26]. Bacal and colleagues demonstrated remodeling of RV after HTx with a reduction in RV volumes and RV mass by cardiac MRI in HTx patients with a mean graft age of 6 years compared with HTx patients with graft age <1 year [1]. The authors suggested that the RV may adapt alterations in PVR after HTx. Our results support these findings, as we demonstrated a good correlation between invasively assessed RV SVI and PAC and also between RV SVI and PVRI. We found that exercise capacity was strongly related to invasively assessed systolic reserve capacity but not to right heart filling pressure alterations. This shows that myocardial deformation capacity and HR reserve are the limiting exercise capacity elements in HTx patients.

The present echocardiographic data indicate that RV diastolic function may be impaired as RV diastolic Doppler parameters were significantly reduced in HTx patients compared with controls. In contrast, the invasive evaluation of right heart filling showed pressures within normal range at rest. We found no correlation between resting invasive and noninvasive right heart filling parameters. However, during exercise, the RV and RA pressures in HTx patients increased to a greater extent than seen in healthy controls in our and previous studies [27]. Caution should therefore be exercised when interpreting RV diastolic Doppler parameters in HTx patients. In contrast, the TR gradient and Nt-ProBNP, which has shown good correlation with LV filling pressure [28], correlated with right heart filling pressure. Even though right heart echocardiographic systolic and diastolic function showed poor relation to invasive right heart pressures, both echocardiographic RV systolic function and right heart pressures correlated with important clinical parameters such as exercise capacity and NYHA functional class. As a result, a comprehensive right heart systolic and diastolic function evaluation should combine invasive RHC with global echocardiographic RV function assessment.

Limitation

We acknowledge a number of limitations to our study. The study reflects the experience of a single center with a limited number of patients. In addition, we do not have information on changes over time due to the cross-sectional design of the study. Further studies are

needed to evaluate the link between RV myocardial perfusion and function, and the remodeling of RV during the early period after transplantation.

Conclusions

Heart transplantation patients have significantly reduced RV systolic function compared with healthy controls. 3D RVEF and 2D longitudinal deformation analyses are associated with clinical performance in stable HTx patients and seem suitable in the noninvasive routine right heart function evaluation after HTx. Invasively assessed RV systolic reserve was strongly associated with exercise capacity. No relation was noted between exercise capacity and right heart filling pressure.

Authorship

TSC: designed and performed the study. Analyzed data and wrote the paper. HE: designed and performed the study and wrote the paper. BBL: designed the study, wrote the paper. MJA: performed the study, analyzed data, and wrote the paper. SM: performed the study and wrote the paper. SHP: designed and performed the study and wrote the paper.

Funding

Funding was received from Health Research Fund of Central Denmark Region and the Danish Heart Association.

Conflicts of interest

The authors have declared no conflicts of interest.

Acknowledgements

Lene Lindencrone Konrad is thanked for her valuable assistance during the semi supine bicycle stress tests.

REFERENCES

1. Bacal F, Pires PV, Moreira LF, *et al.* Normalization of right ventricular performance and remodeling evaluated by magnetic resonance imaging at late follow-up of heart transplantation: relationship between function, exercise capacity and pulmonary vascular resistance. *J Heart Lung Transplant* 2005; **24**: 2031.
2. Stobierska-Dzierzek B, Awad H, Michler RE. The evolving management of acute right-sided heart failure in cardiac transplant recipients. *J Am Coll Cardiol* 2001; **38**: 923.
3. Wahl A, Feller M, Wigger E, *et al.* Pretransplant pulmonary hypertension and long-term allograft right ventricular function. *Eur J Cardiothorac Surg* 2010; **37**: 61.
4. Butler J, Stankewicz MA, Wu J, *et al.* Pre-transplant reversible pulmonary hypertension predicts higher risk for mortality after cardiac transplantation. *J Heart Lung Transplant* 2005; **24**: 170.
5. Chang PP, Longenecker JC, Wang NY, *et al.* Mild vs severe pulmonary hypertension before heart transplantation: different effects on posttransplantation pulmonary hypertension and mortality. *J Heart Lung Transplant* 2005; **24**: 998.
6. Goland S, Siegel RJ, Burton K, *et al.* Changes in left and right ventricular function of donor hearts during the first year after heart transplantation. *Heart* 2011; **97**: 1681.
7. Fyfe DA, Mahle WT, Kanter KR, Wu G, Vincent RN, Ketchum DL. Reduction of tricuspid annular doppler tissue velocities in pediatric heart transplant patients. *J Heart Lung Transplant* 2003; **22**: 553.
8. Lunze FI, Colan SD, Gauvreau K, *et al.* Cardiac allograft function during the first year after transplantation in rejection-free children and young adults. *Circ Cardiovasc Imaging* 2012; **5**: 756.
9. Lang RM, Badano LP, Mor-Avi V, *et al.* Recommendations for cardiac chamber quantification by echocardiography in adults: an update from the American Society of Echocardiography and the European Association of Cardiovascular Imaging. *Eur Heart J Cardiovasc Imaging* 2015; **16**: 233.
10. Verhaert D, Mullens W, Borowski A, *et al.* Right ventricular response to intensive medical therapy in advanced decompensated heart failure. *Circ Heart Fail* 2010; **3**: 340.
11. Guendouz S, Rappeneau S, Nahum J, *et al.* Prognostic significance and normal values of 2D strain to assess right ventricular systolic function in chronic heart failure. *Circ J* 2012; **76**: 127.
12. Antoni ML, Scherptong RW, Atary JZ, *et al.* Prognostic value of right ventricular function in patients after acute myocardial infarction treated with primary percutaneous coronary intervention. *Circ Cardiovasc Imaging* 2010; **3**: 264.
13. Hardegree EL, Sachdev A, Villarraga HR, *et al.* Role of serial quantitative assessment of right ventricular function by strain in pulmonary arterial hypertension. *Am J Cardiol* 2013; **111**: 143.
14. Cappelli F, Porciani MC, Bergesio F, *et al.* Right ventricular function in AL amyloidosis: characteristics and prognostic implication. *Eur Heart J Cardiovasc Imaging* 2012; **13**: 416.
15. Seldinger SI. Catheter replacement of the needle in percutaneous arteriography; a new technique. *Acta Radiol* 1953; **39**: 368.
16. Andersen MJ, Borlaug BA. Invasive hemodynamic characterization of heart failure with preserved ejection fraction. *Heart Fail Clin* 2014; **10**: 435.
17. Noble BJ, Borg GA, Jacobs I, Ceci R, Kaiser P. A category-ratio perceived exertion scale: relationship to blood and muscle lactates and heart rate. *Med Sci Sports Exerc* 1983; **15**: 523.
18. Mehra MR, Crespo-Leiro MG, Dipchand A, *et al.* International Society for Heart and Lung Transplantation working formulation of a standardized nomenclature for cardiac allograft vasculopathy-2010. *J Heart Lung Transplant* 2010; **29**: 717.

19. Stewart S, Winters GL, Fishbein MC, *et al.* Revision of the 1990 working formulation for the standardization of nomenclature in the diagnosis of heart rejection. *J Heart Lung Transplant* 2005; **24**: 1710.
20. Raichlin E, Edwards BS, Kremers WK, *et al.* Acute cellular rejection and the subsequent development of allograft vasculopathy after cardiac transplantation. *J Heart Lung Transplant* 2009; **28**: 320.
21. Tamborini G, Muratori M, Brusoni D, *et al.* Is right ventricular systolic function reduced after cardiac surgery? A two- and three-dimensional echocardiographic study. *Eur J Echocardiogr* 2009; **10**: 630.
22. Eleid MF, Caracciolo G, Cho EJ, *et al.* Natural history of left ventricular mechanics in transplanted hearts: relationships with clinical variables and genetic expression profiles of allograft rejection. *JACC Cardiovasc Imaging* 2010; **3**: 989.
23. D'Andrea A, Riegler L, Nunziata L, *et al.* Right heart morphology and function in heart transplantation recipients. *J Cardiovasc Med (Hagerstown)* 2013; **14**: 648. doi: 10.2459/JCM.0b013e32835ec634.
24. Clemmensen TS, Logstrup BB, Eiskjaer H, Poulsen SH. Changes in longitudinal myocardial deformation during acute cardiac rejection: the clinical role of two-dimensional speckle-tracking echocardiography. *J Am Soc Echocardiogr* 2015; **28**: 330.
25. Clemmensen TS, Logstrup BB, Eiskjaer H, Hoyer S, Poulsen SH. The long-term influence of repetitive cellular cardiac rejections on left ventricular longitudinal myocardial deformation in heart transplant recipients. *Transpl Int* 2015; **28**: 475. doi: 10.1111/tri.12520.
26. Butler CR, Kim DH, Chow K, *et al.* Cardiovascular MRI predicts 5-year adverse clinical outcome in heart transplant recipients. *Am J Transplant* 2014; **14**: 2055.
27. van Empel VP, Kaye DM, Borlaug BA. Effects of healthy aging on the cardiopulmonary hemodynamic response to exercise. *Am J Cardiol* 2014; **114**: 131.
28. Iwanaga Y, Nishi I, Furuichi S, *et al.* B-type natriuretic peptide strongly reflects diastolic wall stress in patients with chronic heart failure: comparison between systolic and diastolic heart failure. *J Am Coll Cardiol* 2006; **47**: 742.